Lab on a Chip

PAPER

Cite this: *Lab Chip*, 2018, **18**, 662

Pressure-actuated monolithic acrylic microfluidic valves and pumps†

Pablo E. Guevara-Pantoja, Rocío J. Jiménez-Valdés, Jose L. García-Cordero * and Gabriel A. Caballero-Robledo *

In this article, we describe a microfluidic device with embedded valves and pumps made exclusively of layers of acrylic glass. Flat acrylic sheets are carved out with a micromilling machine and bonded together by solvent bonding. The working principle of the valves is based on a thin flexible membrane (≈100 μm) machined on one acrylic sheet and actuated with pneumatic pressure. A completely closed valve resists a pressure difference of ≈17 kPa (≈2.5 psi), and when open, it can sustain flow rates of up to 100 μL s^{-1}. Pumping is achieved by combining two valves and a pumping chamber in series, which is also based on the bending of a thin acrylic membrane. The maximum flow rate obtained with this pumping mechanism is 20 μL min^{-1}. Acrylic is a popular rigid thermoplastic because it is inexpensive, making it ideal for mass production of disposable devices, and also because it has demonstrated compatibility with different biochemical assays. The physical and optical properties it shares with other thermoplastics could lead to this material being implemented for similar valves and pumps. As a proof-of-concept of our technology, we implemented a controlled cell-staining assay in two parallel incubation chambers integrating four valves and one pump into one device. Our monolithic acrylic valves can enable the mass production of disposable microfluidic devices that require fluid control with pressure-actuated valves and aid in the automation of biochemical assays.

Received 13th December 2017,
Accepted 12th January 2018

DOI: 10.1039/c7lc01337j

rsc.li/loc

1 Introduction

There has been mounting interest in both industry and academia to develop microfluidic devices made of plastics because of their amenability to high-volume and fast production rates, as well as their compatibility with different bioassays.[1,2] Thermoplastics are extremely inexpensive materials, ideal for the commercialization of microfluidic devices because they can be manufactured in large volumes at low cost employing a set of replication and direct fabrication techniques, such as injection and compression molding, hot embossing, micro-thermoforming, casting, micro-milling, laser ablation, or plasma etching.[3–6] Examples of thermoplastics include polycarbonate (PC), polystyrene (PS), poly(methyl methacrylate) (PMMA), polypropylene (PP), polyethylene terephthalate (PET), polyvinyl chloride (PVC), and cycloolefin copolymer (COC), among others. In most instances, thermoplastics show superior biochemical compatibility to silicon, glass and PDMS,[3,4] and a wide range of surface chemistry techniques has been optimized for use with most of these thermoplastics.[5]

In general, accessories used in biological and biochemical laboratories are made of rigid thermoplastics: microwell plates are made of PS, vinyl, PMMA, PP, or COC; transwell plate membranes are made of PC and PET; PCR well plates and centrifuge tubes are made of PP; Petri dishes and culture flasks are made of PS and PP, and pipette tips are made of PP. These plastics share similar mechanical, thermal, and optical properties (see Table S1 of the ESI†) and can be manufactured using the aforementioned fabrication techniques. For years, biologists and biochemists have garnered *in vitro* data using accessories made of these plastics – in the case of cell biology, for many decades – thus, using microfluidic devices made of other materials would likely entail re-characterization of cell–material interactions, or adapting their assays and surface chemistries to new materials. This is one of several factors as to why microfluidics has not been fully adopted outside academia, despite its well-known advantages. Yet, translating biochemical assays originally developed for microplates or tubes into thermoplastic microfluidic devices has been relatively straightforward, as has been shown in some cases for capillary electrophoresis,[7] PCR,[8] cell-free protein synthesis,[9] screening of pharmaceutical candidates,[10] cell culture,[11–13] and ELISAs.[14] However, these

Cinvestav-Monterrey, 66600, Apodaca, Nuevo León, Mexico.
E-mail: g.a.caballero.robledo@gmail.com, jlgarciac@cinvestav.mx

† Electronic supplementary information (ESI) available: Document; Video S1: the two-chamber staining system flowing dye into each chamber in a controlled way. See DOI: 10.1039/c7lc01337j

devices consist of simple microchannels or microchambers lacking fluidic control elements; thus, a long-standing milestone in the lab-on-a-chip field has been the development of valves and pumps made exclusively from rigid thermoplastics.

Microvalves and pumps are key components of most microfluidic analytical systems; they help control and regulate flow within microfluidic channels allowing the automation of complex biochemical assay steps. Simple microfluidic channels can be manufactured from virtually any material employing a variety of microfabrication techniques; the most common materials include glass, silicon, polymers, thermoplastics and elastomers. However, the moment microfluidic valves and pumps are integrated into a microfluidic system, its fabrication complexity increases considerably, often because it requires two or more different materials to construct it.[15] One of the most popular microfluidic valves is the pressure-actuated valve. This valve consists of a control and flow layer separated by a thin flexible material (typically an elastomer) such that when the control channel is actuated, the membrane deforms and pinches off or opens the flow channel.[16,17]

There have been continuous efforts to develop microvalves embedded in thermoplastic microfluidic devices, yet all of these devices still rely on a soft membrane made of a material different from the rest of the device.[18–22] Examples of this include membranes made of PDMS,[23–26] Viton,[20] thermoplastic polyurethane,[27,28] fluorinated ethylene–propylene Teflon,[29–31] and Fluorocur perfluoropolyether,[32] which are sandwiched between layers of PMMA, PS, PC, PP, PVC, or COC. However, adding a layer of a different material imposes several restrictions for potential mass fabrication of these devices because of the increased number of assembly steps and, in addition, because it would require adapting different surface chemistries for each of the materials in contact with a solution. Ideally, to facilitate their mass production, microfluidic devices should be made of a single thermoplastic material and be bonded using popular techniques, such as thermal- or solvent-assisted methods. A notable exception, though not entirely a thermoplastic, has been the recent report on a 3D-printed microfluidic valve and pump.[33] It should be noted that the construction of microfluidic devices made exclusively of thermoplastic elastomers[34–37] is compatible with some of the most common mass manufacturing techniques.[36] Yet, to date, demonstration of microfluidic control elements made exclusively of rigid thermoplastics, such as PP, PS or PMMA, and standard materials for labware where biochemical and cellular assays are traditionally performed, has been scarce.[38] Furthermore, developing a working valve or pump using any of these materials may be easily translated to the rest of the rigid thermoplastics.

In this paper, we describe the fabrication, operation and performance of microfluidic valves made entirely of acrylic. We show the integration of several microvalves and a pump into a single device to trap cells into two different chambers. This device demonstrates system complexity in addition to embedding chambers and channels of different heights. Trapped cells were then stained with different dyes and observed under a fluorescence microscope.

2 Materials and methods

Microfabrication

1.3 mm thick acrylic sheets (ME303018, Goodfellow, USA) were drilled using a 3D milling machine (MDX-40A, Roland AG, Germany) with a two-flute, square end mill, 200 μm, drill

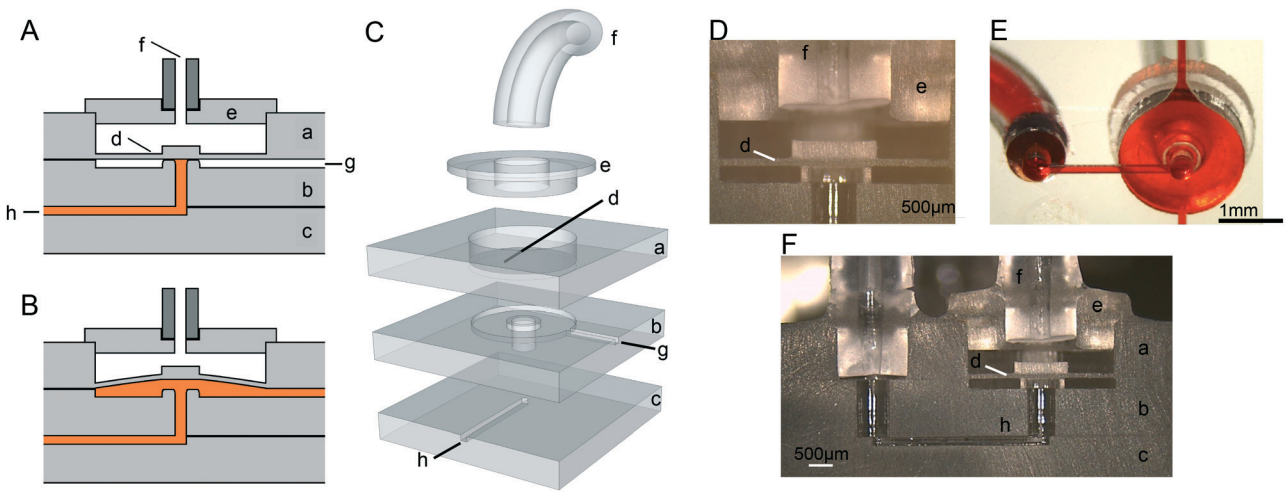

Fig. 1 Schematic representation of a cross-sectional view of the closed (A) and open (B) microfluidic valve. (C) Three-dimensional view of the microvalve. (D) Cutaway of the valve. (E) A photograph from the bottom of the valve filled with red ink. (F) Micrograph of the cutaway of a device showing a valve, microfluidic channels and tubing of image (E). The different parts of the valve indicated in panels (A), (C), (D) and (F) are: a. pneumatic control layer, b. valve flow layer, c. principal flow layer, d. machined acrylic membrane (diameter = 3 mm, thickness = 300 μm in the central part, and 100 μm elsewhere), e. machined acrylic tubing coupling, f. pneumatic control line, g and h. square flow channels (width = depth = 200 μm).

bit (Kyocera, 1600-0080L012). The flow channels were drilled according to the design shown in Fig. 1 on two "flow" sheets (sheets b and c) using a spindle speed of 15 000 rpm and a feed rate of 1 mm s^{-1}. With this method, the minimum width of the channels is limited by the size of the drill bit. Structures as thin as 50 μm can be made with a drill bit of similar size,[39] although they are more fragile. Channel depth is a parameter that is easier to control; we regularly fabricated 200 μm-deep channels but it is possible to make channels as small as 5 μm deep.[40]

The thin flexible membrane is made by drilling a circular pit on a "control" acrylic sheet (sheet a in Fig. 1) using a 0.5 mm drill bit (Kyocera, 1610-0200L060). The diameter of the pit is 3 mm while the thickness of the membrane is 100 μm. Such a small thickness can be achieved thanks to the 2 μm vertical mechanical resolution of the milling machine. In addition, setting the "zero" vertical position (*z*-axis) on the surface of the workpiece table where the acrylic sheets are placed allowed us to achieve almost identical thicknesses, independent of the uniformity of the acrylic sheets. We fabricated twenty membranes on four acrylic pieces and found an average thickness value of 97 μm with a standard deviation of 2 μm. Details of this experiment can be found in the ESI.†

We found that flat membranes were prone to deformation so we increased the thickness to about 300 μm of the region where the membrane makes contact with the rim of the channel below it. The characterization of the deformation of the membrane as a function of membrane thickness is included in the ESI.† We believe that fabricating thinner membranes could be achieved by employing a combination of microfabrication techniques like electroplating and hot embossing.

Holes and tube–sheet coupling (part e in Fig. 1), which connect the plastic tubing to the chip, are made using the 0.5 mm drill bit. The tube–sheet coupling is made with the same kind of acrylic sheet as those used for the rest of the valve. We were able to fabricate five devices like the one reported in Fig. 6B before the drill bit surface started wearing off which thus altered the finish of the micromachining.

Bonding protocol

The machined acrylic sheets are placed on top of a 3 mm-thick glass substrate, which is then positioned inside a Petri dish with the bonding side facing upwards. Everything is placed inside a larger dish partially filled with water (Fig. 2A). Next, the flexible membrane and the valve inlet are covered with small patches of PDMS in order to protect them from being attacked by the solvent and prevent their bonding. One milliliter of chloroform is poured into the Petri dish around the glass sheet without touching the acrylic sheets. The Petri dish is then closed to create an atmosphere saturated with chloroform (Fig. 2B). After three minutes, the Petri dish is opened, the PDMS patches are removed, and the sheets are manually aligned and gently pressed against each other (Fig. 2C). The alignment of the sheets is easily achieved by using aligning structures included in the design, which are schematically represented in Fig. 2. Finally, the system is placed in a home-made mechanical press to apply a pressure of 18 kg cm^{-2} at 85 °C for 15 minutes. This bonding protocol is based on the method reported by Ogilvie *et al.*,[39] and we have added the use of the protective PDMS patches as a crucial element to make the flexible membrane functional. One could imagine that, in scaling up this process, a jig with PDMS patches could be designed such that it is easily aligned with the acrylic sheets in an automated process. Fig. 2 shows the bonding between the control layer and one of the flow layers, however the bonding of a second flow layer employs the same protocol.

An important advantage of this bonding protocol is that the chloroform helps diminish the roughness of the milled channels by "polishing" the surfaces exposed to the solvent and thus increase their optical quality.[39]

Valve set-up

Once the acrylic layers are bonded, the coupling and the external tubing (Tygon, ND-100-80, I.D. 0.02″, O.D. 0.06″) are glued to their corresponding inlets using regular glue (Resistol 911, Henkel). The pneumatic control line (tube f in Fig. 1) is connected to a series of pneumatic valves (MH1, Festo, USA), which in turn are connected to an air compressor set at a manometric pressure of 172 kPa (25 psi) and to a vacuum pump (manometric pressure of ≈−96.5 kPa). The pneumatic valves are controlled using a computer, allowing the microfluidic valves to alternate between applying pressure and vacuum in the chamber above the membrane, thus

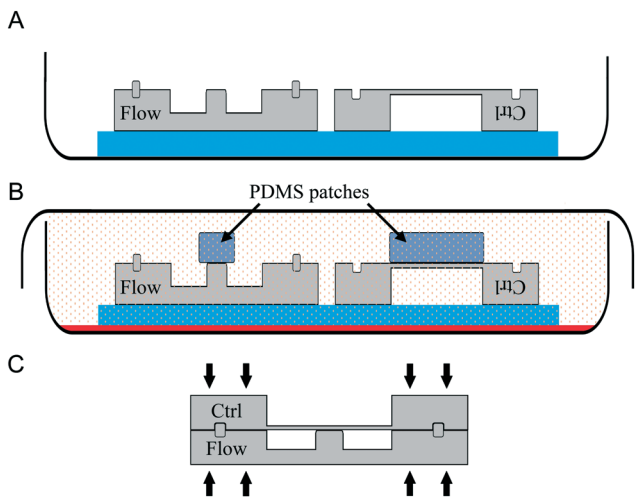

Fig. 2 Bonding protocol. (A) The flow and control sheets are placed on a glass platform inside a Petri dish and, subsequently, everything is placed inside a larger Petri dish partially filled with water. (B) An atmosphere saturated with chloroform is created inside the dish but the flexible membrane and the valve inlet are covered with small patches of PDMS to protect them from being attacked by the solvent. (C) After 3 min, the PDMS patches are removed and the sheets are aligned (using complementary small guides drilled on both sheets) and pressed against each other. A third acrylic sheet can be aligned and bonded later using the same procedure.

opening and closing the microfluidic valve by deflecting the membrane up and down (see Fig. 1).

The vast difference in the microchannel's flow rate when the valve was open or closed upon applying a forward pressure compelled us to use two different methods to measure the flow rate. Large flow rates obtained with the valve open were measured by connecting the outlet of the microchannel through a long tube onto a precision balance: the rate of change of weight registered by the balance gave the flow rate through the valve. Small flow rates generated with the valve closed were measured by monitoring 1 μm polystyrene tracer particles (Fluoresbrite 18660-5, Polysciences, Inc.) flowing in the center of the channel with an optical microscope. We estimated the total flow rate using the relationship between the maximum velocity and flow in a square channel.

Cell staining methods

THP-1 cells, a pro-monocytic cell line, were cultured in RPMI 1640 (21870-076, Thermo Fisher Scientific Inc., USA) supplemented with 10% fetal bovine serum (FBS, 16000-036, Thermo Fisher Scientific Inc., USA), 2 mM L-glutamine (35050-061, Thermo Fisher Scientific Inc., USA), 4500 mg L^{-1} glucose (G8644, Sigma-Aldrich Co., USA), 10 mM HEPES (15630-080, Thermo Fisher Scientific Inc., USA), and 100 nM penicillin/streptomycin (15140-122, Thermo Fisher Scientific Inc., USA). Before performing the experiment, the device was cleaned and sterilized by flowing 70% ethanol; subsequently, the device was filled with RPMI medium. Cells were injected manually with a syringe into the chambers of the device at 1×10^6 cells per mL through the outlets located after the chambers. Since THP-1 cells are not adherent cells, they were allowed to settle at the bottom of the chambers before injecting the stains. Cells in the first chamber were stained with fluorescent calcein AM (ex/em ~495 nm/~515 nm; Thermo Fisher Scientific Inc., USA) to indicate intracellular esterase activity and therefore cell viability. Next, cells in the second chamber were also stained with calcein AM. Finally, the cell nuclei of the second and the first chambers, in that order, were stained with Hoechst 33342 (ex/em ~361 nm/~497 nm, Thermo Fisher Scientific Inc., USA). 2 μM calcein AM and 10 μg mL^{-1} Hoechst were flowed at a rate of 270 μL h^{-1} for 10 min into each chamber independently. The valves of the device were controlled as previously explained. The experiment was performed at room temperature, and cells were observed with a 10× objective. Bright-field and fluorescence micrographs were obtained with a motorized inverted Zeiss microscope (Axio Observer A1, Carl Zeiss Microscopy GmbH, Germany) with a 14-bit monochrome camera (Zeiss Axiocam 506 Mono).

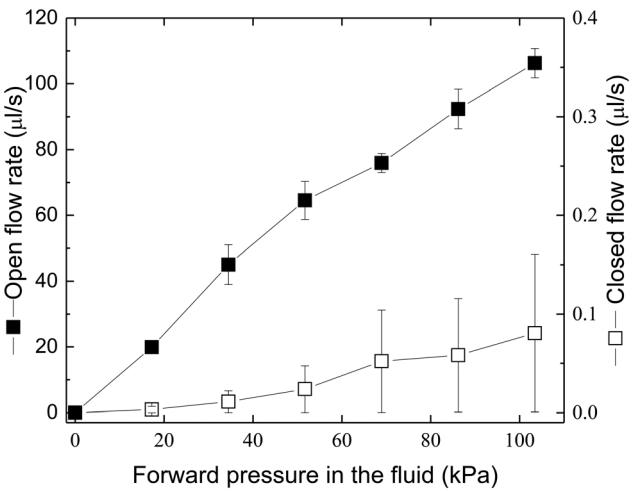

Fig. 3 Flow rate through the valve as a function of the forward fluid pressure. The black squares show a linear relationship between the flow and the pressure when the valve is open. The white squares show that the valve impedes flow without leakage up to a forward pressure of ~20 kPa.

3 Results and discussion

Valve design and performance

Our acrylic microfluidic valves consist of two flow layers and a third layer for pneumatic control. Fig. 1 shows a schematic representation of the cross-section of the closed (A) and open (B) valve, a three-dimensional design (C), and images of a valve (D–F). A microfluidic channel (g) on the upper flow layer (b) is connected to a circular pool, which has a hole in the center with a rim through which fluid can flow in or out of the flowing zone between layers (b) and (c). The rim has the same height as the depth of the microfluidic channel. The pool is covered with a thin 100 μm acrylic membrane (d) which is part of the control layer (a). The central part of the membrane has a thickness of 300 μm to avoid deformation during the fabrication process and improve the sealing of the valve. The empty space above the membrane is closed using a machined tube–sheet coupling (e), which allows its connection to the pneumatic control line with Tygon tubing (f).

When pressure is applied to the pneumatic control line, the membrane is pushed against the ring in the center of the pool and the valve is closed (Fig. 1A). When vacuum is applied, the membrane deforms upwards and the valve opens (Fig. 1B). The mechanical properties of the membrane were reported in our previous work[41] where we found that the membrane has a Hookean elastic constant of $\kappa \approx 7.07 \times 10^4$ N m^{-1}, which corresponds to a maximum displacement of the center of the membrane of ±10 μm when subjected to manometric pressures of ±96.5 kPa (±14 psi).

The geometry and working principle of this valve follow similar principles reported for other PDMS-based microfluidic valves,[22,33,42,43] however our device is entirely made of acrylic. Ordinarily, the membrane is made of a soft material (*e.g.* elastomer), which has the advantage of being able to seal better the valve hole. These valves can resist a forward fluid pressure as high as 45 kPa without leakage,[42] compared to the 17 kPa our valve can sustain, albeit at the cost of increasing fabrication complexity and employing two different materials. The quality of the seal of our valve is affected by the maximum deformation of the membrane (see the ESI†) and

the roughness of the rim. This roughness is the result of the micromilling process, a similar phenomenon which has been observed in pillars fabricated using the same technique.[44] This roughness could be reduced by exposing the rim to a solvent[39] before sealing the device; though in our current protocol, this part of the device is not exposed to the solvent during the bonding protocol because it is covered with a PDMS patch. However, we believe that making these structures by electroplating and hot embossing would eliminate this problem and thus improve the sealing. Overall, the fabrication of our device is less complex and can easily progress to mass production as it consists exclusively of monolithic acrylic parts.

We tested the performance of our microvalve by applying different values of forward liquid pressure and measuring the resulting flow rate, both with the valve open and closed. Fig. 3 shows the resulting flow rate through the microfluidic channel as a function of the forward pressure. When the valve is open, the flow rate scales linearly as a function of pressure. When closed, the valve is capable of resisting a forward liquid pressure of ~17 kPa (~2.5 psi) with it being completely sealed. The inherent rigidity of acrylic is the main limiting factor to the flow rate when the valve is open. The maximum deflection of the membrane could be improved by making a larger membrane or by reducing its thickness, although our fabrication method imposes a limit to the variation of these parameters because the membrane becomes deformed when it is too thin (see the ESI†).

Pump design and performance

A microfluidic pumping system is made by machining two valves on the extremes of a microfluidic channel and a pumping membrane in between (Fig. 4). Compared to a single valve, the pumping membrane does not have a hole and ring in the center of the circular pool in the flow layer. Fig. 4 shows such a pumping system where the valves are connected to microfluidic channels in the second flow layer.

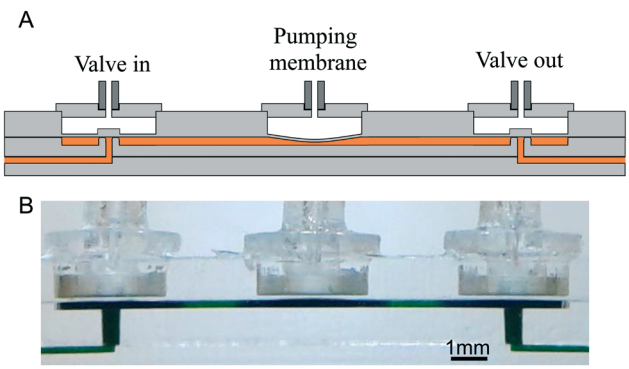

Fig. 4 Two valves and a pumping membrane are connected in series to create a pumping system. A schematic representation of the pump is shown in (A) and a picture of the device filled with green ink is shown in (B). Three acrylic sheets are aligned and bonded together. From top to bottom: the pneumatic control sheet, the pumping flow sheet, and the principal flow sheet.

Both valves and the pumping membrane in Fig. 4 are connected to solenoid valves controlled by a computer, which allows the valves and pumping membrane to alternate simultaneously between pressure and vacuum in the chambers above the flexible membranes. Opening and closing the valves and pushing the flexible membrane up and down in a coordinated way can generate a net flow through the microfluidic channels. Depending on the order in which the chambers are pressurized and de-pressurized, the flow can be directed in either direction. For the particular case of a flow from left to right depicted in Fig. 4, a pumping cycle would consist of the following steps: 1) first, the input valve is opened, the output valve is closed and vacuum is applied to the pumping membrane to pull it up; 2) next, the input valve is closed, the output valve is opened, and pressure is applied to the pumping membrane to push it down. Fig. 5 shows the flow rate generated by the pump as a function of the cycle frequency, which demonstrates that the optimal frequency for our system is between 6.5 and 10 Hz, frequencies at which the maximum flow rate close to 0.4 μl s^{-1} is reached. For larger frequencies, the volume pumped per cycle drops drastically causing the flow rate to also drop, as can be observed in the figure.

Application to differential cell staining

To test the functionality of the valves and the pump and their use in biological assays, we designed and built an integrated acrylic microfluidic device consisting of two cell chambers, four microvalves, and a microfluidic pump. Differential staining of cells is performed in two chambers with two different fluorescent dyes. Fig. 6A depicts a schematic of the device showing all its relevant elements. The device is made with three acrylic sheets drilled, aligned, and bonded together. Fluidic microchannels are machined in two layers of the device and connected by holes. The microfluidic channels

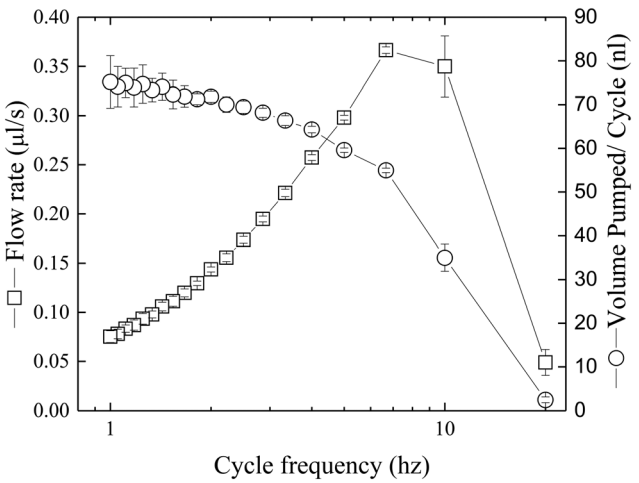

Fig. 5 Flow rate and volume pumped per cycle generated by the pump as a function of the cycle frequency. The optimal cycle frequency is between 6 and 10 Hz where a maximal flow rate of about 0.4 μl s^{-1} is reached.

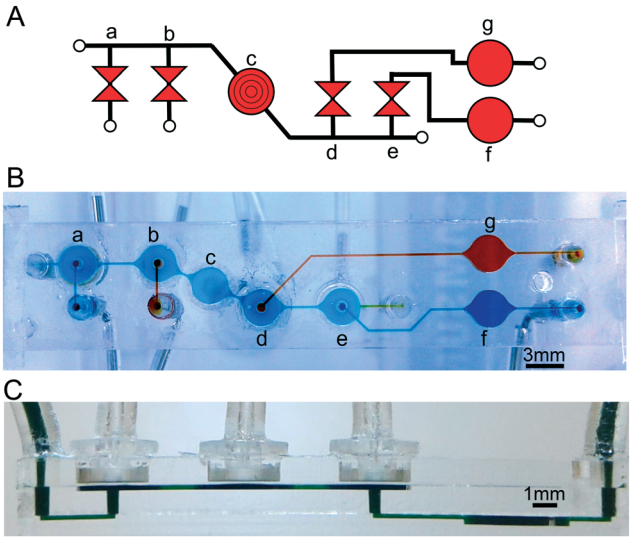

Fig. 6 (A) Design of a two-chamber cell staining system. a. Valve-in 1; b. valve-in 2; c. pumping membrane; d. valve-out 1; e. valve-out 2; f. chamber 1; g. chamber 2. The small dots are connecting holes to external tubes. (B) Picture of the system where blue ink was flowed through chamber 1 and red ink through chamber 2. (C) Lateral picture of a simplified version of the device where only the pump and one chamber were fabricated. The system is filled with green ink. The deeper cell chamber can be seen in the principal flow sheet.

are square, 200 μm per side. To enable the capture of monocytes by sedimentation, the depth of the cell chambers (f and g in Fig. 6) was designed to be deeper than the rest of the microfluidic channels; the chambers had a diameter of 4 mm and a depth of 0.5 mm. Fig. 6B shows a photograph of the microfluidic device where red ink was flowed from left to right through one chamber and blue ink through the other chamber, demonstrating the correct performance of the device (see also Video S1 of the ESI†). A cross-sectional view of a simpler version of the device is shown in Fig. 6C, where only the pump and one cell chamber are shown. The two microfluidic layers and the depth of the chamber can be clearly observed.

Fig. 7(A) shows a schematic representation of the staining protocol and Fig. 7(B) shows both chambers of the device with independent staining for the whole experiment. THP-1 cells were introduced into the chambers and were allowed to settle for 10 min (step 1 in Fig. 7). Next, calcein AM and Hoechst dyes were introduced at different time points using the on-chip pump. First, calcein AM (green) was flowed through the first cell chamber, while the other cell chamber remained closed by actuating its valves (step 2 in Fig. 7). The micrographs in Fig. 7 show that the cells in the closed chamber were left unstained confirming that there was no leakage. Next, the valves in the second chamber were opened and cells were also stained with calcein AM (step 3 in Fig. 7). Then, the valve corresponding to the first chamber was actuated, and the cells in the second chamber were stained with Hoechst (blue), while the cells in the first chamber, already stained with calcein, were left unstained (step 4 in Fig. 7). This

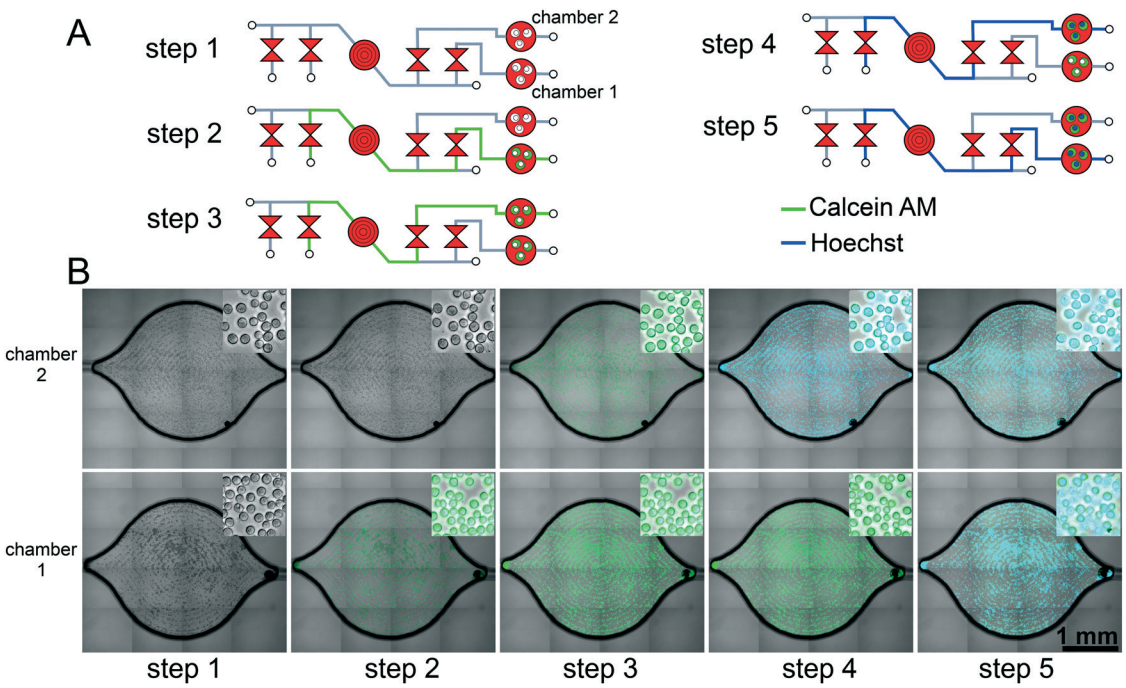

Fig. 7 Acrylic valves and pump allowing differential staining of cells inside the chambers of the device. (A) Schematic representation of the steps followed for differential staining: step 1 - THP-1 cells are introduced into chambers 1 and 2; step 2 - cells in chamber 1 are stained with calcein AM; step 3 - cells in chamber 2 are stained with calcein AM; step 4 - cells in chamber 2 are stained with Hoechst; step 5 - cells in chamber 1 are stained with Hoechst. (B) Micrographs of the chambers of the device with the THP-1 cells after each staining step. The insets show cells in the chambers in regions of ~100 μm per side. More detailed micrographs of the experiment can be found in the ESI.†

corroborated the functionality of both valves. Finally, the cells in both chambers were stained with both Hoechst and calcein at the end of the experiment (step 5 in Fig. 7).

4 Conclusions

The rigid nature of acrylic might give the impression that a microfluidic valve made exclusively of this material could not be achieved. Generally, a pressure-actuated microfluidic valve requires a flexible membrane to open and close a microfluidic channel. The modulus of elasticity of PDMS can reach up to 5 mPa; in contrast, rigid thermoplastics have a Young's modulus that ranges from 1–10 GPa,[37] that is, three orders of magnitude larger. This is probably one of the reasons why soft elastomers have been employed to make pressure-actuated microfluidic valves, but this nevertheless requires other rigid materials to provide support. However, this imposes several restrictions on the types of materials that can be used to seal against the membranes and thus defines the types of bonding techniques to assemble them. Also, surface chemistry for at least two different materials has to be considered for this type of microfluidic device.

In this article, we have shown that thin acrylic membranes can be made flexible enough to build functional microfluidic valves. We also showed that these valves can be fabricated with a regular milling machine and bonded using a combination of solvent and heating pressure. The demonstration of our valves and pumps made exclusively of a thermoplastic paves the road for the development of inexpensive, mass-produced devices with complex functionalities. Although we employed acrylic to fabricate our devices, we believe that the design of our valves and pumps could be adapted to other thermoplastics.

The quality of the sealing when the valve is closed can resist forward liquid pressures up to 17 kPa while the pump can achieve flow rates as high as 20 μL min^{-1}. We were able to integrate several valves and a pump, together with cell culture chambers, into a single device. We used this device to trap cells and stain them, demonstrating the ability of our technology to perform a biochemical assay. One current limitation of our acrylic valve is its comparatively larger size, measuring about 3 mm in diameter. However, by employing other microfabrication techniques, such as electroplating and hot embossing, a decrease in the diameter and the height of the membrane could be attainable.

Veres and coworkers[34–37] have demonstrated microfluidic valves and pumps made entirely of thermoplastic elastomers, materials with similar characteristics to PDMS yet also being thermoplastics, which as such is a very promising technology for producing monolithic microfluidic devices. Whether this new material or the plastics discussed in this article could become the standard, or suitable, material for developing microfluidic devices in industry or academia would ultimately depend on, among others: (i) the type of bioassay to be implemented, (ii) the difficulties in adapting biochemical and cellular assays already well established for materials such as glass and rigid thermoplastics (*i.e.* PS, PP, PC, PMMA) to a new material, (iii) in the case of a new material, the validation of its effects on cellular assays, (iv) the availability of different surface chemistry protocols, (v) the compatibility with different readout techniques, (vi) the facilities and costs with which the material could be adapted to large-scale production techniques, (vii) the availability of rapid prototyping techniques that can quickly translate a prototype into a mass-producible microfluidic device, (viii) the number of steps and complexities required to assemble and bond such a device, and finally, (ix) the availability of fluidic control elements, such as valves and pumps.

Conflicts of interest

There are no conflicts of interest to declare.

Acknowledgements

This work has been supported by CONACyT, Mexico, under Grants 256097 and 262771, and the Fronteras de la Ciencia 2015-2/1178 and 1132. PGP and RJV thank CONACyT for financial support.

References

1 E. Berthier, E. W. K. Young and D. Beebe, *Lab Chip*, 2012, **12**, 1224–1237.
2 D. J. Guckenberger, T. E. de Groot, A. M. D. Wan, D. J. Beebe and E. W. K. Young, *Lab Chip*, 2015, **15**, 2364–2378.
3 A. de Mello, *Lab Chip*, 2002, **2**, 31N–36N.
4 T. D. Boone, Z. H. Fan, H. H. Hooper, A. J. Ricco, H. Tan and S. J. Williams, *Anal. Chem.*, 2002, **74**, 78A–86A.
5 H. Becker and C. Gärtner, *Anal. Bioanal. Chem.*, 2008, **390**, 89–111.
6 H. Becker and C. Gärtner, *Electrophoresis*, 2000, **21**, 12–26.
7 W. Tan, Z. H. Fan, C. X. Qiu, A. J. Ricco and I. Gibbons, *Electrophoresis*, 2002, **23**, 3638–3645.
8 C. G. Koh, W. Tan, M.-Q. Zhao, A. J. Ricco and Z. H. Fan, *Anal. Chem.*, 2003, **75**, 4591–4598.
9 K. Jackson, T. Kanamori, T. Ueda and Z. Hugh Fan, *Integr. Biol.*, 2014, **6**, 781–788.
10 A. J. Ricco, T. D. Boone, Z. H. Fan, I. Gibbons, T. Matray, S. Singh, H. Tan, T. Tian and S. J. Williams, *Biochem. Soc. Trans.*, 2002, **30**, 73–78.
11 M. Raasch, K. Rennert, T. Jahn, S. Peters, T. Henkel, O. Huber, I. Schulz, H. Becker, S. Lorkowski, H. Funke and A. Mosig, *Biofabrication*, 2015, **7**, 015013.
12 E. W. K. Young, E. Berthier, D. J. Guckenberger, E. Sackmann, C. Lamers, I. Meyvantsson, A. Huttenlocher and D. J. Beebe, *Anal. Chem.*, 2011, **83**, 1408–1417.
13 Y. Wang, J. Balowski, C. Phillips, R. Phillips, C. E. Sims and N. L. Allbritton, *Lab Chip*, 2011, **11**, 3089–3097.
14 C. D. Chin, T. Laksanasopin, Y. K. Cheung, D. Steinmiller, V. Linder, H. Parsa, J. Wang, H. Moore, R. Rouse, G. Umviligihozo, E. Karita, L. Mwambarangwe, S. L. Braunstein,

J. van de Wijgert, R. Sahabo, J. E. Justman, W. El-Sadr and S. K. Sia, *Nat. Med.*, 2011, **17**, 1015 EP –.
15 J. L. Garcia-Cordero, D. Kurzbuch, F. Benito-Lopez, D. Diamond, L. P. Lee and A. J. Ricco, *Lab Chip*, 2010, **10**, 2680–2687.
16 W. H. Grover, A. M. Skelley, C. N. Liu, E. T. Lagally and R. A. Mathies, *Sens. Actuators, B*, 2003, **89**, 315–323.
17 M. A. Unger, H.-P. Chou, T. Thorsen, A. Scherer and S. R. Quake, *Science*, 2000, **288**, 113–116.
18 P. Gu, K. Liu, H. Chen, T. Nishida and Z. H. Fan, *Anal. Chem.*, 2011, **83**, 446–452.
19 K. Pitchaimani, B. C. Sapp, A. Winter, A. Gispanski, T. Nishida and Z. Hugh Fan, *Lab Chip*, 2009, **9**, 3082–3087.
20 I. R. G. Ogilvie, V. J. Sieben, B. Cortese, M. C. Mowlem and H. Morgan, *Lab Chip*, 2011, **11**, 2455–2459.
21 B. Cortese, M. C. Mowlem and H. Morgan, *Sens. Actuators, B*, 2011, **160**, 1473–1480.
22 S. A. M. Shaegh, Z. Wang, S. H. Ng, R. Wu, H. T. Nguyen, L. C. Z. Chan, A. G. G. Toh and Z. Wang, *Microfluid. Nanofluid.*, 2015, **19**, 557–564.
23 P. Skafte-Pedersen, C. G. Sip, A. Folch and M. Dufva, *J. Micromech. Microeng.*, 2013, **23**, 055011.
24 K. S. Lee and R. J. Ram, *Lab Chip*, 2009, **9**, 1618–1624.
25 Y. Suzuki, M. Yamada and M. Seki, *Sens. Actuators, B*, 2010, **148**, 323–329.
26 C.-F. Chen, J. Liu, C.-C. Chang and D. L. DeVoe, *Lab Chip*, 2009, **9**, 3511–3516.
27 P. Gu, T. Nishida and Z. H. Fan, *Electrophoresis*, 2014, **35**, 289–297.
28 S. A. M. Shaegh, A. Pourmand, M. Nabavinia, H. Avci, A. Tamayol, P. Mostafalu, H. B. Ghavifekr, E. N. Aghdam, M. R. Dokmeci, A. Khademhosseini and Y. S. Zhang, *Sens. Actuators, B*, 2018, **255**, 100–109.
29 S. Huang, Q. He, H. Chen and J. Huang, *Microfluid. Nanofluid.*, 2013, **14**, 329–335.
30 W. H. Grover, M. G. von Muhlen and S. R. Manalis, *Lab Chip*, 2008, **8**, 913–918.
31 P. A. Willis, B. D. Hunt, V. E. White, M. C. Lee, M. Ikeda, S. Bae, M. J. Pelletier and F. J. Grunthaner, *Lab Chip*, 2007, **7**, 1469–1474.
32 P. A. Willis, F. Greer, M. C. Lee, J. A. Smith, V. E. White, F. J. Grunthaner, J. J. Sprague and J. P. Rolland, *Lab Chip*, 2008, **8**, 1024–1026.
33 A. K. Au, N. Bhattacharjee, L. F. Horowitz, T. C. Chang and A. Folch, *Lab Chip*, 2015, **15**, 1934–1941.
34 J. P. Rolland, R. M. Van Dam, D. A. Schorzman, S. R. Quake and J. M. DeSimone, *J. Am. Chem. Soc.*, 2004, **126**, 2322–2323.
35 G. S. Fiorini, R. M. Lorenz, J. S. Kuo and D. T. Chiu, *Anal. Chem.*, 2004, **76**, 4697–4704.
36 E. Roy, M. Geissler, J.-C. Galas and T. Veres, *Microfluid. Nanofluid.*, 2011, **11**, 235–244.
37 E. Roy, J.-C. Galas and T. Veres, *Lab Chip*, 2011, **11**, 3193–3196.
38 P. Zhou, L. Young and Z. Chen, *Biomed. Microdevices*, 2010, **12**, 821–832.
39 I. R. G. Ogilvie, V. J. Sieben, C. F. A. Floquet, R. Zmijan, M. C. Mowlem and H. Morgan, *J. Micromech. Microeng.*, 2010, **20**, 065016.
40 P. E. Guevara-Pantoja and G. A. Caballero-Robledo, *RSC Adv.*, 2015, **5**, 24635–24639.
41 P. Vázquez-Vergara, A. M. T. Rojas, P. E. Guevara-Pantoja, E. C. Poiré and G. A. Caballero-Robledo, *J. Micromech. Microeng.*, 2017, **27**, 077001.
42 W. Zhang, S. Lin, C. Wang, J. Hu, C. Li, Z. Zhuang, Y. Zhou, R. A. Mathies and C. J. Yang, *Lab Chip*, 2009, **9**, 3088–3094.
43 J. A. Weaver, J. Melin, D. Stark, S. R. Quake and M. A. Horowitz, *Nat. Phys.*, 2010, **6**, 218–223.
44 R. Hernandez-Perez, Z. H. Fan and J. L. Garcia-Cordero, *Anal. Chem.*, 2016, **88**, 7312–7317.